J. Membrane Biol. 173, 73–87 (2000)

The Journal of
Membrane
Biology

Topical Review

Water Permeability Measurement in Living Cells and Complex Tissues

A.S. Verkman
Departments of Medicine and Physiology, Cardiovascular Research Institute, University of California, San Francisco, CA 94143-0521, USA

Received: 3 August 1999/Revised: 22 September 1999

Abstract. The identification of molecular water transporters and the generation of transgenic mice lacking water transporting proteins has created a need for accurate methods to measure water permeability. This review is focused on methodology to characterize water permeability in living cells and complex multicellular tissues. The utility of various parameters defining water transport is critically evaluated, including osmotic water permeability (P_f), diffusional water permeability (P_d), Arrhenius activation energies (E_a), and solute reflection coefficients (σ_p). Measurements in cellular and complex tissues can be particularly challenging because of uncertainties in barrier geometry and surface area, heterogeneity in membrane transporting properties, and unstirred layer effects. Strategies to measure plasma membrane P_f in cell layers are described involving light scattering, total internal reflection fluorescence microscopy, confocal microscopy, interferometry, spatial filtering microscopy, and volume-sensitive fluorescent indicators. Dye dilution and fluorescent indicator methods are reviewed for measurement of P_f across cell and tissue barriers. Novel fluorescence and gravimetric methods are described to quantify microvascular and epithelial water permeabilities in intact organs, using as an example lungs from aquaporin knockout mice. Finally, new measurement strategies and applications are proposed, including high-throughput screening for identification of aquaporin inhibitors.

Key words: Water transport — Aquaporin — Fluorescence — Cell transfection — Transgenic mouse — Microscopy

Correspondence to: A.S. Verkman

Introduction

Fluid transport across cellular barriers is of fundamental importance in animal and plant physiology. Water permeability in some systems is subject to long-term and/or short-term regulation involving transcriptional control, vesicular trafficking and post-translational membrane protein modification. For more than a century water transport measurements have been carried out in various artificial porous membranes and tissues derived from plant and animal sources. The reader is referred to several older treatises for an historical account of early contributions in the field (Dick, 1966; Stein, 1967).

Several recent advances have created the need to reevaluate strategies to characterize water permeability in complex systems and to develop new measurement methods and analysis procedures. The identification of aquaporin and non-aquaporin molecular water transporters has mandated the development of methods for precise measurement of water permeability in heterologous expression systems. The recent generation of transgenic knockout mice deficient in aquaporin water channels (Ma et al., 1997, 1998, 1999) has inspired the development of novel strategies to characterize water transport in complex mammalian tissues and intact organs. The older goal of cataloging water transport parameters has in large part been replaced by hypothesis-driven research to determine whether aquaporin proteins mediate water transport across defined tissue barriers and to elucidate the molecular mechanisms of regulated water transport.

The purpose of this review is to evaluate modern strategies to characterize the water permeability properties of living cells and multicellular tissues. The perspective of this review is more practical than theoretical, emphasizing measurement approaches and analysis procedures that provide clear-cut information about water

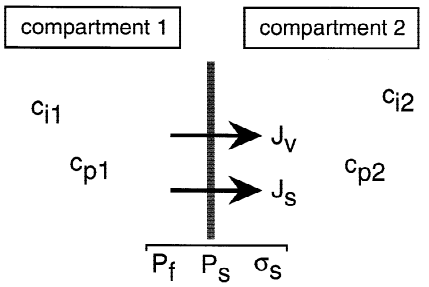

Fig. 1. Water and solute permeability across a single barrier separating compartments 1 and 2. c_{i1} and c_{i2} are the osmolalities of impermeant solutes on sides 1 and 2, and c_{p1} and c_{p2} the osmolalities of permeant solutes. Barrier permeability properties include the osmotic water permeability coefficient P_f, the solute permeability coefficient P_s and the solute reflection coefficient σ_p. Water flux (J_v) and solute flux (J_s) are defined as positive in the left-to-right direction as indicated.

transporting mechanisms. General paradigms for water transport characterization are discussed, and specific examples are provided to demonstrate technical details and limitations.

Parameters Defining Water Permeability

Figure 1 shows a semipermeable membrane separating compartments 1 and 2, each containing one type of impermeant and permeant solute. The volume flow (J_v cm^3/sec) across the membrane is defined by,

$$J_v = P_f S v_w [(c_{i2} - c_{i1}) + \sigma_p(c_{p2} - c_{p1}) + (P_1 - P_2)/RT] \quad (1)$$

where P_f (cm/sec) is the osmotic water permeability coefficient, S (cm^2) the membrane surface area, v_w (18 cm^3/mol) the partial molar volume of water, P the hydrostatic pressure (atm), σ_p the reflection coefficient of the permeant solute, c_{i1} and c_{i2} the osmolalities of impermeant solutes on sides 1 and 2, and c_{p1} and c_{p2} the osmolalities of permeant solutes on sides 1 and 2. J_v is defined as positive in the direction from side 1 to 2. It is assumed in Eq. 1 that the membrane barrier is homogeneous with respect to permeability properties and that P_f, S and σ_p are independent of osmotic gradient size and direction.

The osmotic water permeability coefficient P_f provides the most useful single parameter characterizing the water transporting properties of a defined barrier. P_f relates net volume flux across a barrier to osmotic and hydrostatic driving forces. For simple membrane barriers like planar bilayers, liposomes and cell plasma membranes, the absolute value of P_f provides a useful index about whether water transport is facilitated by molecular pores such as aquaporin water channels. Based on measurements in lipid bilayers and cell systems, P_f greater than 0.01 cm/sec (at 25–37°C) is considered to be high and suggests the involvement of molecular water channels, whereas P_f less than 0.005 cm/sec is consistent with water diffusion through the lipid portion of a membrane. The interpretation of measured P_f in terms of molecular water channels assumes accurate definition of barrier surface area S and the absence of significant unstirred layer effects. As defined by Eq. 1, P_f is measured from the volume flux produced by a defined osmotic gradient or hydrostatic driving force. Much of this review is devoted to biophysical strategies to evaluate P_f across cell membranes and complex cellular barriers.

For water movement through distinct water transporting units such as aquaporin-type water channels, it is useful to define a single channel osmotic water permeability p_f (cm^3/sec) as: $p_f = P_f/n$, where n is the membrane density of functional water channels (number/cm^2). If parallel pore-dependent and independent pathways exist as in many cell plasma membranes, then the pore-independent contribution to P_f must be subtracted for meaningful computation of p_f. The single channel water permeability is useful in making quantitative comparisons of intrinsic water permeability properties, such as for different aquaporins or mutated aquaporins. Single channel water permeabilities are potentially useful in deducing apparent pore sizes when assumptions are made about the details of pore shape. It is often assumed that water channels are smooth right cylindrical pores; for example the measured p_f of 6×10^{-14} cm^3/sec for the AQP1 water channel gives an apparent pore radius of 1.8 nm (Zhang et al., 1993) using equations describing osmosis through narrow single-file pores (Finkelstein, 1987). However, the assumption of a simple cylindrical pore is probably an unjustified oversimplification, so that meaningful interpretation of pore size parameters from permeability data must await atomic resolution structural information and advances in molecular dynamics computations which take into account pore-water interactions.

The Arrhenius activation energy (E_a, kcal/mol) is defined by the relation $ln\ P_f = E_a/RT + A$, where R is the gas constant, T is absolute temperature, and A is an entropic term. E_a is generally determined from the slope of an Arrhenius plot of $ln\ P_f$ *vs.* $1/RT$. E_a provides a measure of the energy barrier to water movement across a membrane. E_a for water movement across a lipid membrane is generally high (>8–10 kcal/mol) because of hydrogen bonding interactions between water and lipid molecules, as well as the lipid dynamics required for creation of a water pathway. For water movement through aqueous channels, E_a is generally found to be low (3–6 kcal/mol). The low E_a associated with water pores is assumed to be related to the weak temperature dependence of water self-diffusion. However, a rigorous theoretical basis for a low E_a in water pores is lacking,

since water movement through molecular water channels probably involves rate-limiting interactions between water molecules and the pore wall rather than water self-diffusion. E_a is also low when P_f is unstirred layer-limited because of the weak temperature dependence of solute diffusion in water. Notwithstanding these caveats, there is some utility in interpreting E_a in terms of water transporting mechanisms across simple barriers. The independence of E_a on surface area (S) can be an advantage in measuring E_a rather than P_f because S may be difficult to determine accurately. It is generally advisable to measure E_a over a wide temperature range in membranes where there may be parallel water transporting pathways having different intrinsic E_a (aquaporin and lipid pathways), and to recognize that nonlinearities in the $ln\ P_f$ *vs.* $1/RT$ relation may arise from numerous complexities such as heterogeneity in water transport properties and temperature-dependent changes in bilayer fluidity. For complex epithelial and multicellular barriers the utility of measuring E_a is questionable. Complex barriers often contain multiple serial and parallel water transporting pathways, each of which may be non-ideal in terms of temperature-independent E_a and osmotic gradient-independent P_f. Also, there can be temperature dependent changes in cell shape due to changes in solute transporter activities and cytoskeletal assembly. However, comparative E_a measurements may be useful in some complex systems, such as intact tissues or organs from control *vs.* aquaporin knockout mice.

The ratio of osmotic-to-diffusional water permeability (P_f/P_d) has been proposed as an independent parameter in providing information about the existence of water pores. The diffusional water permeability coefficient P_d (cm/sec) is defined as the rate of water transport (exchange) across a membrane in the absence of an osmotic gradient,

$$J_{H2O} = P_d\, S\, ([H_2O^*]_1 - [H_2O^*]_2) \qquad (2)$$

where J_{H2O} is the diffusive water flow and $[H_2O^*]$ is the concentration of "labeled" water. Experimental methods for measurement of P_d involving tritiated water flux (Brahm, 1982), nuclear magnetic resonance (Verkman & Wong, 1987; Benga et al., 1993), H_2O/D_2O exchange (Kuwahara & Verkman, 1988; Ye & Verkman, 1989; Iserovich et al., 1997) and other approaches have been reviewed previously (Verkman, 1995). P_f/P_d should theoretically equal unity for simple lipid bilayer membranes that do not contain water channels. P_f/P_d can be greater than unity when water moves through a wide pore or narrow channel, or when measured P_d is less than true membrane P_d because of unstirred layers. Various equations have been derived that relate P_f/P_d to simple pore geometries (Finkelstein, 1987; Hill, 1994), but as mentioned above for pore size determination from single channel water permeabilities, it is unlikely that simplified pore equations can provide useful information about pore geometry. Further, there is probably little or no utility in attempting to measure P_d in systems more complex than liposomes or small suspended cells like erythrocytes. There is compelling evidence that P_d is unstirred layer-limited in epithelia, oocytes, planar lipid membranes and large cells, sometimes by several orders of magnitude (Levine, Jacoby & Finkelstein, 1984; Berry, 1985; Zhang & Verkman, 1991; Folkesson et al., 1996; Carter et al., 1996). Because of its limited utility P_d will not be discussed further in this review.

The final parameter to be considered is the solute reflection coefficient σ_p. The flux (J_s, mol/sec) of an uncharged permeant solute (c_p) across the simple barrier in Fig. 1 is given by,

$$J_s = P_s\, S\, (c_{p1} - c_{p2}) + J_v\, (1 - \sigma_p)\, \langle c_p \rangle \qquad (3)$$

where P_s (cm/sec) is the solute permeability coefficient and $\langle c_p \rangle$ is the 'mean solute concentration' in the pore. Equations 1 and 3 (Kedem & Katchalsky, 1958) are derived from non-equilibrium thermodynamics and so are formally valid for small osmotic and solute gradients. For charged solutes, the equations are modified to include electro-osmotic phenomena. The second term in Eq. 3 defines the solvent drag of a solute with σ_p less than unity. Equations 1 and 3 have been numerically integrated for specific geometries in studies involving σ_p determination (Levitt & Mlekoday, 1983; Pearce & Verkman, 1989; Shi, Fushimi & Verkman, 1991; Yang & Verkman, 1998). σ_p has been measured experimentally by induced osmosis and solvent drag strategies as reviewed previously (Verkman et al., 1996). Induced osmosis involves the measurement of J_v in response to osmotic gradients created by an impermeant *vs.* test solute as defined by Eq. 1. Solvent drag involves the measurement of J_s in the absence and presence of forced osmosis as defined by Eq. 3.

The reflection coefficient has been used in evaluating whether a common water-solute transporting pathway exists. σ_p is defined by the relation, $\sigma_p = 1 = P_s v_s / P_f v_w - f$, where v_s is the partial molar volume of solute and f is a 'frictional' term arising from water-solute interactions in a water pore. Values of σ_p less than unity ($f > 0$) have been taken as evidence for a common water/solute pathway, provided that $P_s v_s / P_f v_w$ is appropriately evaluated. However σ_p should be interpreted with caution in biological systems. σ_p determination can be exceedingly difficult technically because of the presence of coupled and uncoupled water and solute transport. Rapid solute diffusion causes an underestimation of σ_p in induced osmosis measurements because of osmotic gradient dissipation by solute diffusion. σ_p is also generally underestimated in solvent drag measurements because of solute movement by both diffusive and

solvent drag mechanisms. In addition, a variety of method-dependent artifacts exist in σ_p determination. There are several cases in the literature where widely different σ_p values have been reported by different laboratories at different times. In human erythrocytes, increasing σ_{urea} value from 0.6–1 have been reported over the past 30 years; the recent molecular identification of distinct water and urea transporting proteins in erythrocytes indicates that σ_{urea} should be near unity. There is an even greater conceptual concern in measuring and interpreting σ_p in biological systems. The σ_p concept and validation were done on artificial porous membranes containing very long narrow macroscopic water conduits containing many millions of water molecules. Because the concentration of water is ~55 molar and solute concentration is generally <1 molar, it is unlikely that a molecular water pore, such as an aquaporin water channel, would contain even one solute molecule at any instant. The concept of solute reflection coefficient in biological systems thus mandates reconsideration. For these technical and theoretical reasons the determination of σ_p in complex biological systems probably has little or no value.

Water Transport Across Cell Plasma Membranes

Water transport across the limiting membrane of a cell or sealed membrane vesicle or liposome is measured from the time course of cell volume change in response to an osmotic challenge. The problem of water permeability determination is thus a problem of cell volume measurement. Various volume-dependent physical parameters have been used to develop strategies for measurement of membrane water permeability. In unlabeled cells, increased cell volume is often accompanied by small changes in light scattering. Cytoplasmic dilution due to cell swelling also causes a decrease in cytoplasmic refractive index which can be exploited by laser interferometry and spatial filtering microscopy. Direct 3-dimensional cell shape reconstruction by brightfield confocal microscopy is theoretically possible, but probably not practical because of poor contrast and scattering from intracellular structures. Additional measurement possibilities are offered by labeling cells with fluorescent dyes. Dilution of an aqueous-phase fluorescent dye distributed in the cytoplasmic compartment can be measured by total internal reflection fluorescence microscopy, confocal fluorescence microscopy or wide-field fluorescence microscopy with appropriate optics to create partial confocality. It is also possible to exploit 'cell volume-sensitive' fluorescent indicators in which integrated cell fluorescence provides a direct measure of cell volume. Labeling of cell plasma membranes with lipid phase dyes affords the possibility of cell shape reconstruction by confocal microscopy. Single particle tracking methods have been applied to study cell swelling and shrinking by labeling the cell surface with bright fluorescent microspheres (Kao & Verkman, 1994). The Table summarizes key features of these strategies, as well as their applicability to measurements on adherent *vs.* suspended cells, polarized epithelial sheets, and heterogeneous cell populations. Further methodological details and examples of water permeability measurements are provided below.

Light Scattering

Light scattering is a well-established method to measure osmotic water permeability in osmotically responsive liposomes, sealed membrane vesicles and some small cells. Light scattering was initially applied to water permeability measurements in erythrocytes (Mlekoday, Moore & Levitt, 1983), and subsequently in membrane vesicles, liposomes reconstituted with water channels, and cell suspensions (Verkman, Dix & Seifter, 1985; van Hoek & Verkman, 1992; Dobbs et al., 1998). The method is based on the dependence of elastically scattered light (Rayleigh scattering) on cell volume. Experimentally, a cell suspension is mixed rapidly with an anisosmotic solution (generally hypertonic) to create a transmembrane osmotic gradient. Osmotic water flux produces a change in cell volume and scattered light intensity. P_f is computed from the light scattering time course, cell surface-to-volume ratio, and an empirically determined relation between light scattering and cell volume (Verkman et al., 1985). It is not practical to compute the dependence of scattered light intensity on cell volume because of complexities in cell shape, optical configuration, and interference phenomena. The light scattering method is simple to apply and very small samples are required; however, there are potential problems in quantitative data interpretation, including cell/vesicle size heterogeneity, motion artifacts just after mixing which occur before flow stops, refractive index changes producing anomalous scattering signals, and in cells, unstirred layers, and scattering from intracellular structures. Light scattering has limited applications in larger and more complex cells. The use of additives (e.g., dextrans) to prevent settling of large cells can be helpful. Light scattering was used recently to show that immunoisolated type I alveolar epithelial cells from lung have the highest water permeability of any mammalian cell membrane studied to date (Dobbs et al., 1998). Because of the concerns mentioned above and uncertainties in type I cell surface-to-volume ratio, P_f in the Dobbs et al. study was confirmed by light-scattering measurements in small sealed membrane vesicles isolated from the type I cells.

Light scattering has also been applied to study osmotically induced changes in volume in adherent cells

Table. Measurement of osmotic water transport across cell plasma membranes

Method	Difficulty	Quantitative	Instrument cost	Suspended cells	Adherent solid support	Polarized cell layers	Comments
Unlabeled cells							
Confocal microscopy	++++	Yes	$$$$	No	Yes	?	Not generally practical
Light scattering	+	No	$	Yes	Yes	?	Simple, but useful in few systems and not reliable
Interferometry	++++	No	$$	No	Yes	Yes	Very difficult experimentally
Spatial filtering	++	No	$	No	Yes	Yes	Simple and accurate, may not work in all systems
Fluorescent cells—cytoplasmic labeling							
Confocal microscopy	++	Yes	$$$$	No	Yes	Yes	Difficult technically
Partial confocality	+	No	$	No	Yes	Yes	Simple, but not consistently reliable
Total internal reflection	++	Yes	$$	No	Yes	No	Reproducible and quantitative, moderate technical difficulty
Volume indicator	+	No	$	Yes	Yes	Yes	Simple, but imperfect signal specificity
Fluorescent cells—membrane labeling							
Confocal microscopy	+++	Yes	$$$$	No	Yes	?	Not generally practical
Fluorescent bead—labeled cells							
Single particle tracking	+++	No	$$$	No	Yes	?	Difficult, assumes simple shape changes

(Fischbarg et al., 1989; Echevarria et al., 1992). Like measurements in suspended cells, light scattering in adherent cells depends in a complex way on cell geometry, the arrangement of illumination and detection optics, intracellular refractive index, and other difficult-to-quantify factors. Nevertheless, in some cell types like J774 macrophages, light scattering provides a simple approach to measure water permeability, provided that appropriate experiments are done to prove that light-scattering signals represent authentic changes in cell volume. Experimentally, a laser beam is directed at a cell layer in which scattered light is measured using an objective lens and detector. The angle and wavelength of the incident beam is empirically optimized to maximize volume-dependent changes in light scattering. Although light-scattering measurements are simple to set up for measurements in adherent cells, in our experience they are useful in a very limited number of cell types and fraught with artifactual signals that are unrelated to changes in cell volume.

Confocal Microscopy

Several optical approaches can be applied to measure the concentration of an aqueous-phase fluorophore in cytoplasm. Cell-loadable fluorescent dyes are available with various properties and wavelengths, such as cell-permeable calcein derivatives that undergo intracellular de-esterification and trapping. Since intracellular fluorophore concentration is inversely related to cell volume, osmotic water permeability can be measured from the time course of cytoplasmic fluorophore concentration in response to osmotic gradients. Wide-field fluorescence measurements in suspended or adherent cells cannot provide information about intracellular fluorophore concentration since cell-integrated fluorescence (proportional to the total number of fluorophores in the light beam) is independent of cell volume. Confocal microscopy using high magnification objectives in principle permits determination of fluorophore concentration because the detected signal arises from a defined volume slab (minimum thickness ~0.5 μm). Because rapid measurements in living cells are required with minimal photobleaching, Nipkow wheel-type confocal microscopes are potentially superior to laser-scanning instruments. The limited *z*-resolution and imperfect point-spread-function of confocal microscope optics may impose limitations in data quality, particularly in thin cell layers. Two-photon fluorescence excitation (Piston, 1999) with wide-field optics should provide similar information about cytoplasmic fluorophore concentration without the need for confocal optics and with minimal photobleaching. Relatively turbid and thick tissues should be amenable for study because two-photon fluorescence is excited by a pulsed infrared source such as a pumped titanium-sapphire laser. Alternatively, semi-quantitative information about cytoplasmic fluorophore concentration can be obtained using partial confocal optics in which the *z*-point spread

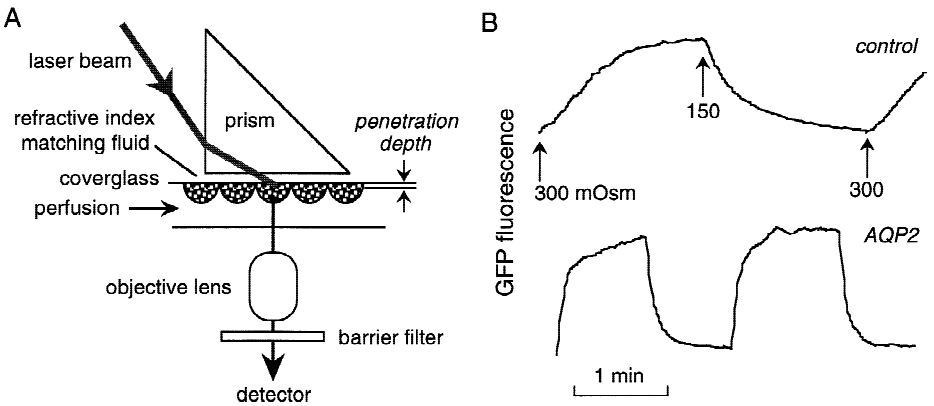

Fig. 2. Measurement of osmotic water permeability in adherent cells by total internal reflection fluorescence microscopy. (*A*) Cells are loaded with a membrane impermeant volume marker. A thin (50–200 nm) layer of cytosol (labeled "penetration depth") is illuminated by a laser beam directed through a glass prism at a subcritical illumination angle. As the cell shrinks in response to an osmotic gradient, fluorophore concentration in the illuminated region increases, producing an increase in detected signal. (*B*) Time course of TIRFM fluorescence in CHO cells after transient transfection with cytoplasmic green fluorescent protein (GFP) alone (control) or together with cDNA encoding AQP2 water channels. GFP provides a volume marker in the transfected cells. Perfusate osmolality was changed as indicated to create osmotic gradients. (Adapted from Tamarappoo and Verkman (1998)).

function of a wide-field optical system is sharpened by use of a high numerical aperture objective and a limiting aperture in the back focal plane of the emission path (Muallem et al., 1992). Despite their potential utility in making quantitative P_f measurements in heterogeneous cell populations and polarized cell sheets, confocal methods have been used little to measure cell water permeability.

Total Internal Reflection Fluorescence Microscopy

Total internal reflection fluorescence microscopy (TIRFM) provides another approach to measure the concentration of an aqueous-phase fluorophore in cytoplasm. TIRFM involves the excitation of fluorophores in membrane-adjacent cytosol near a high-to-low refractive index interface (Ölveczky, Periasamy & Verkman, 1997). Fluorescence excitation is usually accomplished using a laser source and glass prism to illuminate the sample at a subcritical angle at a glass-aqueous interface (Fig. 2*A*). It is not difficult to equip a conventional epifluorescence microscope with a laser source and prism to make TIRFM measurements. Cells are loaded with an aqueous-phase dye. Cell swelling in response to an osmotic gradient results in cytosolic fluorophore dilution and decreased fluorescence signal (Farinas, Simenak & Verkman, 1995). Cell shrinkage produces increased TIRFM fluorescence. Because the effective depth of TIRFM illumination (<150–200 nm) is much smaller than cell thickness (and much smaller than possible by confocal microscopy), TIRF provides a quantitative and relatively simple approach to monitor relative cell volume in adherent cells of arbitrary shape and size. In addition, fluorophore photobleaching in TIRF is minimal because a small fraction of total cell volume is illuminated and fluorophores diffuse rapidly in cytoplasm (Kao, Abney & Verkman, 1993). Signal detection is carried out using photomultiplier or avalanche photodiode detectors, or by camera detectors if P_f values are needed in separate cells in a heterogeneous cell population. Because cells must be cultured on a solid transparent support for TIRFM, it is not possible to measure apical *vs.* basolateral membrane permeabilities in polarized cell sheets.

TIRFM has been applied to measure osmotic water permeability in cells transfected with the vasopressin-regulated water channel AQP2 (Katsura et al., 1995; Valenti et al., 1996). Addition of cAMP agonists produces exocytic plasma membrane insertion of functional AQP2 water channels and increased osmotic water permeability. TIRFM was used to measure water permeability in individual microdissected skeletal muscle fibers that were loaded with a fluorescent dye and immobilized on a polylysine-coated coverglass (Frigeri et al., 1998). TIRFM can also be used to measure water permeability in cells expressing cytoplasmic green fluorescent protein (GFP) in the aqueous-phase cytoplasm. In a study from our laboratory, water permeability was measured in transiently transfected cells coexpressing GFP and wildtype *vs.* mutant AQP2 water channels (Tamarappoo & Verkman, 1998). Even with imperfect transfection efficiency, water permeability could be measured selectively in the fluorescent cells coexpressing AQP2. Figure 2*B* shows increased osmotic water permeability in AQP2 transfected *vs.* control cells. The ability to target GFP to se-

lected cell types opens up a number of interesting possibilities, such as water permeability measurements in GFP-targeted tissues in transgenic mice.

Methods Based on Volume-Dependent Changes in Cell Refractive Index

Cell swelling causes dilution of cytoplasmic proteins and solutes producing a small change in intracellular refractive index. Doubling of cell volume in cultured mammalian cells decreased refractive index from 1.367 to 1.405; cell shrinking by 50% increased refractive index to 1.347 (Farinas & Verkman, 1996). Measurement of intracellular refractive index would thus provide a direct index of relative cell volume in unlabeled cell layers on solid or transparent supports, or epithelial tissues such as amphibian urinary bladder. A proof-of-principle study was done utilizing laser interferometry (Farinas & Verkman, 1996) in which changes in intracellular refractive index were quantified by measurement of the small changes in optical pathlength of a laser beam passing through a cell layer. The approach was formally validated using an interferometry microscope. Plasma membrane P_f was measured in cultured epithelial cells and intact toad urinary bladder. Although technically elegant, interferometry is not practical for routine use because of the requirement for specialized optical instrumentation, the need for constant temperature, vibration-free facilities, and the challenging task of laser beam alignment.

A simple method to exploit the dependence of intracellular refractive index on cell volume was subsequently developed utilizing spatial filtering Fourier optics. Spatial filtering is the optical principle responsible for contrast generation in phase contrast and darkfield microscopes. Interference of zero order (non-scattered) and phase-shifted first order (scattered) beams produce image contrast as depicted in Fig. 3*A*. A rigorous mathematical basis for this phenomenon as applied to cells is reported in Farinas et al. (1997). With the appropriate arrangement of optics, the intensity of transmitted monochromatic light provides a semi-quantitative measure of cell volume. The spatial filtering method was used to measure water permeability in aquaporin transfected cells grown on solid supports, and apical *vs.* basolateral membrane water permeabilities in epithelial cells and intact toad urinary bladder (Farinas et al., 1997). Figure 3*B* shows the time course of transmitted light intensity in a phase contrast microscope for primary cultures of human tracheal epithelial cells grown on porous supports. Apical and basolateral membrane water permeabilities were deduced from light transmittance signal changes (proportional to volume changes) produced by changes in osmolality of the perfusate bathing the apical or basolateral surfaces. Determination of absolute P_f requires an appropriate mathematical description as reported in the Farinas et al. paper which takes into account the 3-compartment nature of an epithelial cell layer. The spatial filtering method is simple to implement and provides excellent quality data in unlabeled cell layers during one-sided or two-sided perfusion.

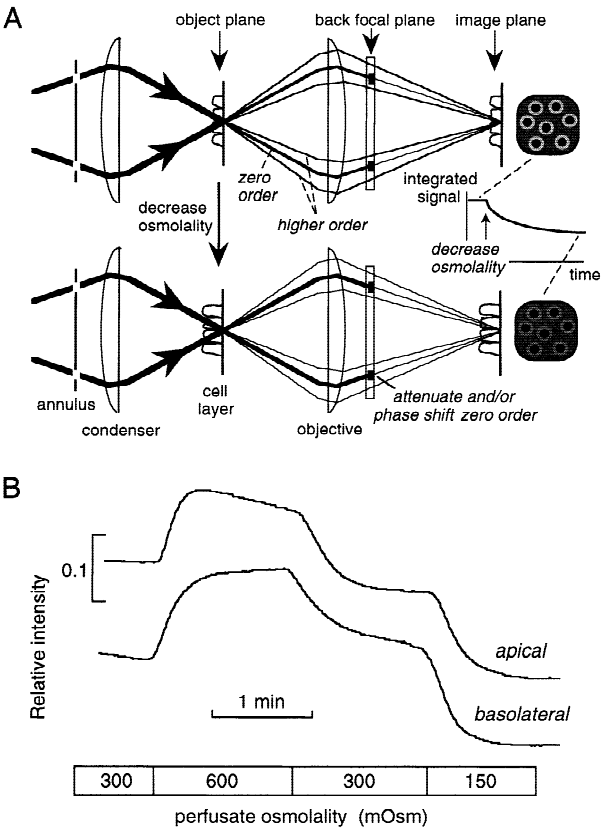

Fig. 3. Measurement of osmotic water permeability in cell layers by spatial filtering transmittance light microscopy. (*A*) Physical principles. Light passing through an annulus is focused at the object plane. The undeflected zero-order beam is attenuated and/or phase-shifted in the back focal plane so as to enhance contrast by interference with scattered higher-order beams. The integrated transmitted light signal is sensitive to cell volume because swelling produces a redistribution of light in zero- *vs.* higher-order beams. (*B*) Osmotic water permeability measured in apical and basolateral plasma membranes of human tracheal epithelial cells in primary culture grown on a porous support. Where indicated osmolality of the perfusate bathing the cell apical or basolateral membranes was changed. For apical/basolateral perfusion, the osmolality of solution bathing the basolateral/apical membrane was maintained at 300 mOsm. Transmitted light intensity provides a semi-quantitative index of cell volume. *See* text for explanations. (Adapted from Farinas et al. (1997)).

Volume-Sensitive Fluorescent Dyes

Direct cell volume read-out using a volume-sensitive fluorescent indicator would provide a simple and accurate approach to measure water permeability in hetero-

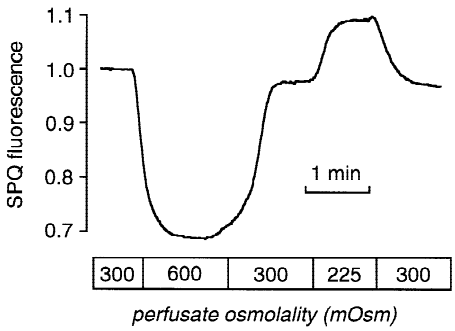

Fig. 4. Measurement of osmotic water permeability using the cell volume-sensitive fluorescent indicator SPQ. CHO cells expressing water channel AQP1 were loaded with SPQ and perfused continuously with solutions of indicated osmolalities. Total cell SPQ fluorescence was measured by wide-field epifluorescence microscopy. Cell volume changes cause quenching (shrinking) or dequenching (swelling) of SPQ fluorescence because of concentration or dilution, respectively, of cytoplasmic contents (Adapted from Jayaraman et al. (1999)).

geneous and polarized cell layers. Previously, a fluorescence quenching method was introduced to measure water permeability in liposomes and vesicles in which the readout was volume-sensitive fluorescence quenching (Chen, Pearce & Verkman, 1988). However available fluorescent indicators cannot be loaded into living cells at high enough concentrations (>1 mM) to make fluorescence quenching possible. We evaluated a series of cell-loadable fluorophores whose fluorescence quantum yield is sensitive to the concentration of endogenous cytoplasmic contents. The chloride-sensitive indicator SPQ was found to be quenched strongly by cytoplasmic organic anions and proteins by a collisional mechanism which conferred volume-dependent fluorescence (Chao et al., 1989). SPQ has been used extensively to measured anion transport in living cells and tissues (reviewed in Mansoura et al., 1999). Figure 4 shows rapid osmotically induced changes in SPQ fluorescence in CHO cells expressing AQP1 water channels. Perfusion with a hyperosmolar solution produces cell shrinking, concentration of cytoplasmic contents, and decreased SPQ fluorescence. SPQ has been used to follow regulatory volume decreases in osmotically challenged cells (Srivinas et al., 1997). Recently, a bright cell trappable anion indicator was introduced, LZQ (Jayaraman et al., 1999), whose fluorescence is quenched by exogenously added iodide. We have successfully used LZQ to measure water permeability in various cells after iodide loading. Water permeability measurements using volume-sensitive fluorescent indicators require only conventional wide-field fluorescence microscopy and can be carried out in complex tissue geometries. However, appropriate control experiments should be done to confirm that changes in fluorescence are related to changes in cell volume. For example, slow changes in cellular SPQ fluorescence after an osmotic challenge can be produced by chloride transport across the cell plasma membrane. Unfortunately, selective cell volume-dependent fluorescent indicators have not been identified to date.

Water Permeability in *Xenopus* Oocytes

An important system for measurement of water permeability is the *Xenopus* oocyte (~0.12 cm diameter), which is the principal system for heterologous water channel expression. Because of mechanical limitations in oocyte swelling, better than 0.1% accuracy in volume measurement with 1 sec time resolution is required. The original swelling assay involved dilution of the extracellular solution with distilled water, and estimation of oocyte volume by measurement of two orthogonal oocyte diameters on a video monitor every 1–5 min (Fischbarg et al., 1990). An improved quantitative imaging approach was subsequently developed in which the shadow cast by an oocyte was recorded and digitized using transmission light microscopy (Zhang & Verkman, 1991). Relative oocyte volume was computed from cross-sectional area (assumed to be proportional to $[\text{volume}]^{2/3}$) by image masking and pixel summation. This approach has been utilized extensively to study new water channel cDNAs, to test whether various transporting proteins contain aqueous pores, and to quantify single channel water permeabilities of aquaporins (Yang & Verkman 1997). A recent advance in the design of an oocyte perfusion chamber permitted analysis of early oocyte volume changes in response to solute gradients (Meinild, Klaerke & Zeuthen, 1998).

Water Transport Across Cell Layers

The methods described above for determination of cell membrane water permeability involve transient measurements of cell volume in response to rapidly imposed osmotic gradients. Often it is necessary to measure net water permeability across a tissue barrier, such as in cultured epithelia, kidney tubules and bladder sacs. Measurement of steady-state osmotic water transport across a tissue barrier generally involves determination of the volume that has moved across the barrier in response to a continuously imposed osmotic gradient. Several approaches are applicable depending upon barrier geometry, required time resolution, and water permeability. The classical gravimetric method is useful for large tissues sacs such as toad urinary bladder, where serial measurements of sac weight provide a quantitative index of time-integrated water movement across the limiting barrier. Imaging methods to quantify sac volume are suitable for P_f measurements in smaller tissue sacs

such as mouse gallbladder. For planar bilayers mounted in Ussing-type chambers, several strategies are applicable to deduce osmotically induced water flux from changes in volume on either side of the barrier. Last, tailored measurement methods have been developed for transepithelial water permeability measurements for specialized tissue geometries such as cylindrical kidney tubules and lung airways as described below.

Water Transport Across Planar Tissue Sheets

For cultured cells grown on porous supports or flat tissue sheets (e.g., cornea, epidermis) mounted in an Ussing-type chamber, osmotically induced volume flow is deduced from the disappearance of water on one side of the barrier and/or the appearance of water on the opposite side. Osmotic gradients or hydrostatic forces are applied using appropriate solutions or pressure differences. A classical method to deduce water flow is to directly read reservoir volume using a thin open capillary tube in continuity with one of the chambers. When water transport rates are high and time resolution is not needed, water flux can be deduced from the concentration of a membrane-impermeant volume marker (e.g., ^{131}I-albumin, FITC-dextran) in one of the chambers. This method has been used to measure transepithelial water flow in AQP2-transfected epithelial cells grown on porous supports in 6-well plastic dishes (Deen et al., 1997). Capacitance probes have been used to measure small changes in reservoir volume in Ussing chambers in challenging applications where flow rates are low or good time resolution is needed. The capacitance method has been used to measure vasopressin-regulated water transport in transfected epithelial cells and planar fragments of amphibian urinary bladder (Toriano et al., 1998), and near-isosmolar water transport in primary cultures of airway epithelial cells (Jiang et al., 1993). It should also be possible to deduce changes in water content of an appropriately small chamber using a membrane-impermeant fluorescent indicator and confocal or TIRFM signal detection as described above.

Water Transport in Perfused Cylindrical Tubules

For cylindrical epithelial cell layers such as kidney tubules, P_f has been measured by in vitro microperfusion using a membrane-impermeant volume marker perfused through the lumen. In the presence of a perfusion bath-to-lumen osmotic gradient, transepithelial P_f is determined from perfused *vs.* collected concentrations of the volume marker, lumen flow, lumen and bath osmolalities, and tubule length and surface area (Al-Zahid et al., 1977). A fluorescence method to measure marker concentration (without the need for collection of luminal fluid) was developed in which a membrane-impermeant fluorescent indicator such as FITC-dextran was used as the luminal volume marker (Kuwahara et al., 1988). Steady-state osmotic water movement out of the lumen produces a progressive increase in fluorophore concentration along the lumen axis that is measurable by wide-field fluorescence microscopy. This method provided an accurate real-time measurement of P_f in perfused kidney collecting ducts (Kuwahara et al., 1990), outer medullary vasa recta (Turner & Pallone, 1997) and distal airways (Folkesson et al., 1996).

Gravimetric and Imaging Methods in Tissue Sacs

The classical gravimetric method to measure osmotically induced transepithelial water transport in amphibian urinary bladder sacs involves serial measurements of sac weight. The principal limitations of gravimetry are the uncertainty in the amount of fluid adhering to the external tissue sac when removed from bathing medium for weight determination, and the accuracy in weight determination. Weight differences of under 10 micrograms (10 nanoliters fluid) can be measured with modern balances positioned on vibration-reducing tables. Additional technical issues, such as the time required to remove the sac from bathing fluid for weight determination and the difficult in handling very small sacs probably limit the utility of classical gravimetry to the measurement of rapid water transport in large tissue sacs such as amphibian urinary bladder. Image analysis to deduce sac volume, as done for *Xenopus* oocytes, provides an alternative approach to quantify sac fluid accumulation. Our laboratory has measured water permeability in small (1.5–2 mm diameter) sacs of mouse gallbladder created by dividing an intact gallbladder using 8-0 Nylon ophthalmic suture (*unpublished data*). As done for oocytes, gallbladder swelling in response to immersion in hypotonic saline was quantified by image analysis. This approach may be useful for water permeability measurements in artificially created sacs of thin tissue layers.

Water Transport in Complex Tissues and Intact Organs

Because of the many possible ways to assemble multiple cell types in a living tissue or whole organ, there are no clear-cut prescriptions to perform and analyze water permeability measurements. The principal challenges in complex tissues are defining the geometry and effective surface area of the barrier(s) to water transport, and determining the effects of unstirred layers on measured water fluxes. One type of complex barrier is that in multilayer tissues such as cornea or epidermis. The degree

to which water moves between cells in this type of barrier can have a major effect on water permeability properties. Another type of barrier is an epithelium-interstitium-endothelium in lung or organs carrying out fluid secretion or absorption. Water movement involves at least three distinct compartments separated by serial barriers with different permeabilities and permselectivity properties. Using the lung as an example, two general approaches, surface fluorescence and gravimetry, are described which provide quantitative permeability data. Other general approaches to quantify water movement in complex tissues include wet-to-dry weight determination, as used recently in transgenic mice for measurements of hydrostatic lung permeability (Bai et al., 1999) and brain edema (Manley et al., 1999), and volume marker dilution in fluid cavities, as used recently in transgenic mice to measure osmotically induced water transport across the peritoneal barrier (Yang et al., 1999).

As mentioned several times in this review, unstirred layer effects are an important concern in water permeability measurements. Because of space limitations and the methodological focus of this review, a rigorous mathematical treatment of unstirred layers is not presented; the reader is referred to an excellent review by Barry and Diamond (1984) in which the issues are systematically developed. For osmotic water movement, unstirred layers result from solute polarization in which convective solute movement (e.g., "sweeping away effects") decreases the effective osmotic gradient across a barrier, producing an underestimate in P_f. Unstirred layers can be extracellular and/or intracellular, and manifest in both transient and steady-state measurements. In the extreme case where P_f is 'unstirred layer-limited', water transport rates are determined by the details of the unstirred layer and not intrinsic barrier properties. In general, unstirred layer effects are greatest for rapid water movement through thick, poorly stirred compartments; however, unstirred layer effects are possible and should be considered in all osmotic water permeability measurements. We have found several experimental strategies to be useful in identifying unstirred layer effects. If artificially increasing barrier water permeability results in an appropriate increase in P_f, then a lower limit to the resistance conferred by unstirred layers can be established. Amphotericin B was used to increase barrier water permeability in *Xenopus* oocytes (Zhang & Verkman, 1991), perfused airways (Folkesson et al., 1996) and the in vivo perfused colon (Wang et al., 1999) to demonstrate minimal unstirred layer effects on osmosis. Another approach is to examine the effect of stirring or perfusion flow rate on P_f. Barrier P_f should not depend on stirring rates; however, it is noted that stirring is not effective in ruling out intracellular unstirred layers or unstirred layers associated with complex extracellular processes such as microvilli. E_a determination can be informative if high, since low E_a (<6 kcal/mol) can be produced by a pore-containing water pathway or unstirred layers. For water permeability measurements in intact organs, capillary perfusion is generally essential to avoid unstirred layer-limited P_f, as described recently for colon P_f measurements in wildtype *vs.* AQP4 knockout mice (Wang et al.,1999).

Osmotic Water Permeability Measurements in Intact Lung

The movement of fluid between the airspace and vascular compartments in lung plays an important role in a number of processes, including the maintenance of a hydrated airway, the reabsorption of alveolar fluid in the neonatal period, and the resolution of pulmonary edema. Folkesson et al. (1994) estimated the P_f between the airspace and capillary compartments in the *in situ* perfused sheep lung using an airspace "instillation and sample" approach. The equilibration of airspace fluid osmolality was measured after infusion of hypertonic saline via the trachea. The equilibration half-time was ~45 seconds, corresponding to a high airspace-capillary P_f of ~0.02 cm/sec. The rate of osmotic equilibration was reversibly slowed by ~3-fold upon addition of $HgCl_2$. It was concluded that water movement between the airspace and capillary compartments in the intact lung was transcellular and facilitated by mercurial-sensitive water channels.

For studies in small animals, where rapid airspace fluid instillation and sampling is not practical, a pleural surface fluorescence method was developed in which airspace osmolality is deduced from the fluorescence of an indicator dissolved in the airspace fluid (Carter et al., 1996). The principle of the method is shown in Fig. 5*A*. The airspace is filled with fluid containing a membrane-impermeant fluorophore and the pulmonary artery is perfused with solutions of specified osmolalities. Because of the finite penetration depth of the excitation light, only lung tissue within 100–200 microns of the pleural surface is illuminated. Under these conditions, the surface fluorescence signal is directly proportional to the airspace fluorophore concentration. In response to an osmotic gradient, water flows between the airspace and perfusate compartments, resulting in a change in fluorophore concentration which is "sampled" by measurement of pleural surface fluorescence. This approach has the advantage of excellent time resolution without the need for invasive sampling. As shown in Fig. 5*B*, the pleural surface fluorescence signal is very stable and the data contain remarkably little experimental noise. In response to doubling of perfusate osmolality from 300 to 600 mOsm, the pleural surface fluorescence signal approximately doubles as predicted theoretically. P_f in

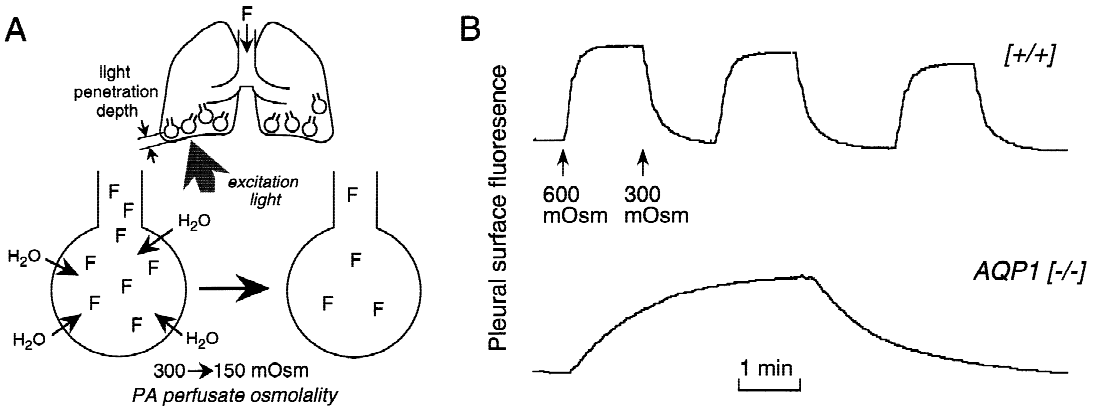

Fig. 5. Airspace-to-capillary osmotic water permeability in intact lung measured by a pleural surface fluorescence method. (*A*) The airspace is filled with saline containing a membrane-impermeant fluorescent probe (*F*) and pleural surface fluorescence is monitored by epifluorescence microscopy ("excitation light"). In response to a decrease in osmolality in fluid perfused into the pulmonary artery, water moves into the airspace and dilutes the fluorophore. Surface fluorescence provides a quantitative measure of intra-alveolar fluorophore concentration. (*B*) Time course of pleural surface fluorescence in mouse lung. The airspace was filled with isosmolar saline containing FITC-dextran and the pulmonary artery was perfused with solutions of indicated osmolalities. Pleural surface fluorescence was monitored continuously by epifluorescence microscopy. Top curve, lung from wildtype mice; bottom curve, lung from AQP1 knockout mouse. (Adapted from Bai et al. (1999)).

mouse lung was 0.017 cm/sec at 23°C, independent of the solute used to induce osmosis, independent of osmotic gradient size and direction, weakly temperature-dependent, and inhibited by $HgCl_2$. The pleural surface fluorescence method was used in a developmental study to show a significant increase in airspace-to-capillary water permeability within the first 24 hr after birth (Carter et al., 1997), and in measurements of lung water transport in aquaporin knockout mice (Bai et al., 1999; Ma et al., 2000). Figure 5*B* shows a ~10-fold decrease in airspace-capillary water permeability in lungs from mice lacking AQP1, a water channel expressed in lung microvascular endothelium.

A strategy was developed to measure microvascular endothelial water permeability in intact lung (Carter et al., 1998). The airspace is filled with an inert, water-insoluble perfluorocarbon to restrict lung water to two compartments—the interstitium and capillaries, and thus establish a single rate-limiting permeability barrier—the capillary endothelium. The pulmonary artery is perfused with solutions of specified osmolalities containing equal concentrations of high molecular weight fluorescein-dextran. In response to a change of perfusate osmolality, water is osmotically driven into or out of the capillaries, resulting in fluorophore dilution or concentration, respectively. The change in fluorophore concentration is recorded as a prompt change (decrease for fluorophore dilution) in pleural surface fluorescence. The magnitude of the prompt deflection in fluorescence signal increases with increased water permeability or decreased pulmonary artery flow. The prompt deflection is followed by a slower return of fluorescence signal to the original level as interstitial and capillary osmolalities equilibrate. Utilizing a 3-compartment model to compute capillary P_f from the fluorescence data, microvascular P_f was found to be ~0.03 cm/sec, weakly temperature-dependent, and inhibited by mercurials. These general strategies should be applicable in measuring P_f in various other organs.

Capillary Filtration in Intact Organs

There is considerable interest in water permeability across microvascular endothelial beds in intact organs, both osmotically driven and hydrostatically driven (filtration) water transport. There is a considerable body of literature using gravimetric determination of lung weight in dogs and other large animals to study capillary filtration (Gaar et al., 1967; Ehrhard et al., 1984). Lung weight includes the sum of fluids contained in the airspace, interstitial and capillary compartments. We recently adapted this classical gravimetric method to measure osmotic water permeability and filtration in mouse lungs (Song et al., 2000). Figure 6*A* shows the apparatus in which lung weight is measured during perfusion. When the airspace compartment is filled with isosmolar saline, changes in perfusate osmolality result in water movement across endothelial and epithelial barriers, which produce changes in the water content of both the interstitial and airspace compartments observed as changes in lung weight. Figure 6*B* (top) shows representative gravimetric data in which decreasing perfusate osmolality from 300 to 250, 200 and 150 mOsm produced an increase in lung weight as water is added to the extravascular spaces of the lung. Figure 6*B* (bottom)

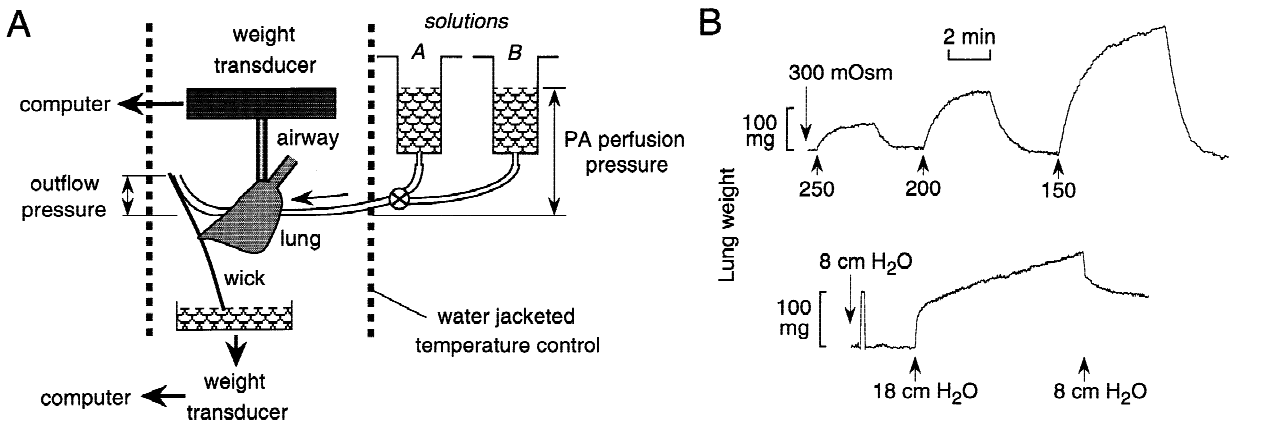

Fig. 6. Gravimetric measurement of lung water permeability. (*A*) Apparatus for continuous measurement of lung weight during perfusion. The airspace compartment is filled with air or saline, and the pulmonary artery perfused with solutions of specified osmolality (solutions *A* and *B*) at specified pulmonary artery (PA) perfusion and outflow pressures. Lung weight is measured continuously by a gravimetric transducer and perfusate exit via the outflow catheter is measured by a second transducer. (*B*) (top) Measurement of osmotic water permeability. Lung weight was recorded continuously in response to indicated changes in perfusate osmolality. The airspace was filled with isosmolar saline and perfusion pressure was 20 cm H_2O. (bottom) Measurement of hydrostatic 'filtration'. Venous outflow pressure was set at 5 cm H_2O and pulmonary artery perfusate pressure was increased from 8 to 18 cm H_2O without change is perfusate osmolality. (Adapted from Song et al. (2000)).

shows a filtration study in which the pulmonary artery was continuously perfused with saline and the pulmonary artery pressure was increased from 8 to 18 cm H_2O at a constant left atrial pressure of 5 cm H_2O. The increased pressure produced a prompt increase in lung weight due to vascular engorgement, followed by a further approximately linear increase in lung weight due to fluid filtration. Preliminary studies suggest that gravimetry is applicable for measurement of microvascular water permeability properties in other organs and tissues.

Perspective and Directions

Several methods to measure osmotic water permeability have been described based on distinct biophysical principles. The selection of suitable measurement methods depends upon the details of the cell/tissue to be studied, the required measurement accuracy, and the need to resolve heterogeneity in water transporting properties from cell-to-cell and in contralateral membranes of polarized cells. However technical advances in cell volume measurement may not overcome fundamental limitations imposed by the geometry of complex tissues and unstirred layer effects. Where absolute water permeability coefficients and activation energies cannot be evaluated with confidence, comparative measurements may be informative, such as comparing transfected *vs.* control cells, or tissues/cells obtained from knockout *vs.* control mice.

A potentially important application of water permeability measurements is in high-throughput screening to identify water channel inhibitors. Studies in aquaporin knockout mice have revealed multiple phenotypic abnormalities, including defective urinary concentrating ability in AQP1 and AQP3 null mice, defective saliva production in AQP5 null mice, abnormal cerebral water balance in AQP4 null mice, defective dietary fat processing in AQP1 null mice, and very low lung water permeability in AQP1 and AQP5 null mice (for review, *see* Verkman, 1998, 1999). We proposed that aquaporin blockers might have clinical applications as aquaretics in hypertension and congestive heart failure, inhibitors of brain swelling following head trauma or stroke, modulators of pulmonary edema, and regulators of increased intracranial and intraocular pressure. The only known compounds that inhibit water/solute transport in some of the aquaporins are mercurial sulfhydryl-reactive compounds which are very toxic and nonspecific. High-throughput screening of tens of thousands to millions of compounds generated by combinatorial chemistry has become a major strategy in drug discovery. High-throughput screening of combinatorial libraries for water channel inhibitors is in progress using aquaporin-transfected cells (Tamarappoo et al., 1999). Of the methods described in this review, confocal microscopy, spatial filtering microscopy, and volume-sensitive fluorescent indicator methods are readily adapted to perform automated water permeability measurements using microplate readers equipped with appropriate optics.

Further advances in water transport measurement strategies will be driven by the continued identification of novel molecular water transporters and regulatory mechanisms, as well as the expanding availability of transgenic mouse models. The measurement of instantaneous volume flow across a membrane or a water channel protein might provide a fundamentally new strategy

to examine the possibility of water channel gating and microheterogeneity in membrane water transporting properties. One possible approach for detection of instantaneous volume flow is to exploit convection-diffusion effects in which the location of a membrane-tethered fluorescent dye functions as a local flow sensor. Improved cell volume sensing methods are needed for the demanding water transport measurements required for high-throughput screening and in vivo studies. Two-photon fluorescence excitation might represent a significant advance in this regard. Refinements are needed in the mathematical modeling of water transport phenomena in complex cellular geometries in order to extract the maximum information content from experimental data. Finally, with the availability of multiple aquaporin knockout mice, approaches will be needed to quantify water transport and fluid dynamics in complex mammalian fluid compartments in vivo, such as the anterior chamber in the eye and the cerebrospinal fluid space in the central nervous system.

This work was supported by grants DK43840, DK35124, HL60288 and HL59198 from the National Institutes of Health, and a grant from the National Cystic Fibrosis Foundation.

References

Al-Zahid, B., Schafer, J.A., Troutman, S.L., Andreoli, T.E. 1977. Effect of antidiuretic hormone on water and solute permeation, and the activation energies of these processes in mammalian cortical collecting tubules. *J. Membrane Biol.* **31:**103–129

Bai, C., Fukuda, N., Song, Y., Ma, T., Matthay, M.A., Verkman, A.S. 1999. Lung fluid transport in aquaporin-1 and aquaporin-4 knockout mice. *J. Clin. Invest.* **103:**555–561

Barry, P.H., Diamond, J.M. 1984. Effects of unstirred layers on membrane phenomena. *Physiol. Rev.* **64:**763–872

Benga, G., Matei, H., Borza, T., Porutiu, D., Lupse, C. 1993. Comparative nuclear magnetic resonance studies of water diffusional permeability of red blood cells from mice and rats. *Comp. Biochem. Physiol.* **104:**491–495

Berry, C.A. 1985. Characteristics of water diffusion in the rabbit proximal convoluted tubule. *Am. J. Physiol.* **249:**F729–F738

Brahm, J. 1982. Diffusional water permeability of human erythrocytes and their ghosts. *J. Gen. Physiol.* **79:**791–819

Carter, E.P., Matthay, M.A., Farinas, J., Verkman, A.S. 1996. Transalveolar osmotic and diffusional water permeability in intact mouse lung measured by a novel surface fluorescence method. *J. Gen. Physiol.* **108:**133–142

Carter, E.P., Ölveczky, B.P., Matthay, M.A., Verkman, A.S. 1998. High microvascular endothelial water permeability in mouse lung measured by a pleural surface fluorescence method. *Biophys. J.* **74:**2121–2128

Carter, E.P., Umenishi, F., Matthay, M.A., Verkman, A.S. 1997. Developmental changes in alveolar water permeability in perinatal rabbit lung. *J. Clin. Invest.* **100:**1071–1078

Chao, A.C., Dix, J.A., Sellers, M.C., Verkman, A.S. 1989. Fluorescence measurement of chloride transport in monolayer cultured cells: mechanisms of chloride transport in fibroblasts. *Biophys. J.* **56:**1071–1081

Chen, P.Y., Pearce, D., Verkman, A.S. 1988. Membrane water and solute permeability determined quantitatively by self-quenching of an entrapped fluorophore. *Biochemistry* **27:**5713–5719

Deen, P.M., Rijss, J.P., Mulders, S.M., Errington, R.J., van Baal, J., van Os, C.H. 1997. Aquaporin-2 transfection of Madin-Darby kidney cells reconstitutes vasopressin-regulated transcellular osmotic water transport. *J. Am. Soc. Nephrol.* **8:**1493–1501

Dick, D.A.T. 1966. Cell Water. Buttesworth, Washington

Dobbs, L., Gonzalez, R., Matthay, M.A., Carter, E.P., Allen, L., Verkman, A.S. 1998. Highly water-permeable type I alveolar epithelial cells confer high water permeability between the airspace and vasculature in rat lung. *Proc. Natl. Acad. Sci. USA* **95:**2991–2996

Echevarria, M., Verkman, A.S. 1992. Optical measurement of osmotic water transport in cultured cells: evaluation of the role of glucose transporters. *J. Gen. Physiol.* **99:**573–589

Ehrhard, J.C., Granger, W.M., Hofman, W.F. 1984. Filtration coefficient obtained by stepwise pressure elevation in isolated dog lung. *J. Appl. Physiol.* **56:** 862–867

Farinas, J., Kneen, M., Moore, M., Verkman, A.S. 1997. Plasma membrane water permeability of cultured cells and epithelia measured by light microscopy with spatial filtering. *J. Gen. Physiol.* **110:**283–296

Farinas, J., Simenak, V., Verkman, A.S. 1995. Cell volume measured in adherent cells by total internal reflection microfluorimetry: application to permeability in cells transfected with water channel homologs. *Biophys. J.* **68:**1613–1620

Farinas, J., Verkman, A.S. 1996. Measurement of cell volume and water permeability in epithelial cell layers by interferometry. *Biophys. J.* **71:**3511–3522

Finkelstein, A. 1987. Water Movement through Lipid Bilayers, Pores, and Plasma Membranes: Theory and Reality. New York, Wiley & Sons

Fischbarg, J., Kunyan, K., Vera, J.C., Arant, S., Silverstein, S., Loike, J., Rosen, O.M. 1990. Glucose transporters serve as water channels. *Proc. Natl. Acad. Sci. USA* **87:**3244–3247

Fischbarg, J., Kunyan, K., Hirsch, J., Lecuona, S., Rogozinski, L., Silverstein, S., Loike, J. 1989. Evidence that the glucose transporter serves as a water channel in J774 macrophages. *Proc. Natl. Acad. Sci. USA* **86:**8397–8401

Folkesson, H., Matthay, M.A., Frigeri, A., Verkman, A.S. 1996. High transepithelial water permeability in microperfused distal airways: evidence for channel-mediated water transport. *J. Clin. Invest.* **97:**664–671

Folkesson, H.G., Matthay, M.A., Hasegawa, H., Kheradmand, F., Verkman, A.S. 1994. Transcellular water transport in lung alveolar epithelium through mercurial-sensitive water channels. *Proc. Natl. Acad. Sci. USA* **91:**4970–4974

Frigeri, A., Nicchia, G.P., Verbavatz, J.M., Valenti, G., Svelto, M. 1998. Expression of aquaporin-4 in fast-twitch fibers of mammalian skeletal muscle. *J. Clin. Invest.* **102:**695–703

Gaar, K.A., Taylor, A.E., Owens, L.J., Guyton, A.C. 1967. Pulmonary capillary pressure and filtration coefficient in the isolated perfused lung. *Am. J. Physiol.* **213:**910–914

Hill, A.E. 1994. Osmotic flow in membrane pores of molecular size. *J. Membrane Biol.* **137:**197–203

Iserovich, P., Kuang, K., Chun, T., Fischbarg, J. 1997. A novel method to determine the diffusional water permeability of oocyte plasma membranes. *Biol. Cell* **89:**293–297

Jayaraman, S., Teitler, L., Skalski, B., Verkman, A.S. 1999. Long-wavelength iodide-sensitive fluorescent indicators for measurement of functional CFTR expression in cells. *Am. J. Physiol.* **277:**C1008–C1018

Jiang, C., Finkbeiner, W.E., Widdicombe, J.H., McCray, P.B., Miller, S.S. 1993. Altered fluid transport across airway epithelium in cystic fibrosis. *Science* **262:**424–427

Kao, H.P., Abney, J.R., Verkman, A.S. 1993. Determinants of the translational diffusion of a small solute in cell cytoplasm. *J. Cell Biol.* **120:**175–184

Kao, H.P., Verkman, A.S. 1994. Tracking of single fluorescent particles in three dimensions: use of cylindrical optics to encode particle position. *Biophys. J.* **67:**1291–1300

Katsura, T., Verbavatz, J.M., Farinas, J., Ma, T., Ausiello, D.A., Verkman, A.S., Brown, D. 1995. Constitutive and regulated membrane expression of aquaporin-CHIP and aquaporin-2 water channels in stably transfected LLC-PK1 cells. *Proc. Natl. Acad. Sci. USA* **92:**7212–7216

Kedem, O., Katchalsky, A. 1958. Thermodynamic analysis of the permeability of biological membranes to nonelectrolytes. *Biochim. Biophys. Acta* **27:**229–246

Kuwahara, M., Berry, C.A., Verkman. A.S. 1988. Rapid development of vasopressin-induced hydroosmosis in kidney collecting tubules measured by a new fluorescence technique. *Biophys. J.* **54:**595–602

Kuwahara, M., Verkman, A.S. 1988. Direct fluorescence measurement of diffusional water permeability in the vasopressin-sensitive kidney collecting tubule. *Biophys. J.* **54:**587–593

Levine, S.D., Jacoby, M., Finkelstein, A. 1984. The water permeability of toad urinary bladder: I. Permeability of barriers in series with the luminal membrane. *J. Gen. Physiol.* **83:**529–541

Levitt, D.G., Mlekoday, H.J. 1983. Reflection coefficient and permeability of urea and ethyleneglycol in the human red cell membrane. *J. Gen. Physiol.* **81:**239–254

Ma, T., Fukuda, N., Song, Y., Matthay, M.A., Verkman, A.S. 2000. Lung fluid transport in aquaporin-5 knockout mice. *J. Clin. Invest.* (*in press*)

Ma, T., Song, Y., Gillespie, A., Carlson, E.J., Epstein, C.J., Verkman, A.S. 1998. Defective secretion of saliva in transgenic mice lacking aquaporin-5 water channels. *J. Biol. Chem.* **274:**20071–20074

Ma, T., Verkman, A.S. 1999. Aquaporin water channels in gastrointestinal physiology. *J. Physiol.* **517:**317–326

Ma, T., Yang, B., Gillespie, A., Carlson, E.J., Epstein, C.J., Verkman, A.S. 1997. Generation and phenotype of a transgenic knock-out mouse lacking the mercurial-insensitive water channel aquaporin-4. *J. Clin. Invest.* **100:**957–962

Ma, T., Yang, B., Gillespie, A., Carlson, E.J., Epstein, C.J., Verkman, A.S. 1998. Severely impaired urinary concentrating ability in transgenic mice lacking aquaporin-1 water channels. *J. Biol. Chem.* **273:**4296–4299

Manley, G.T., Fujimura, M., Ma, T., Feliz, F., Bollen, A., Chan, P., Verkman, A.S. 1999. Aquaporin-4 deletion in mice reduces brain edema following acute water intoxication and ischemic stroke. *J. Am. Soc. Nephrol.* **10:**20*A* (*Abstr.*)

Mansoura, M., Biwersi, J., Ashlock, M., Verkman, A.S. 1999. Fluorescent chloride indicators to assess the efficacy of CFTR cDNA delivery. *Human Gene Therapy* **10:**861–875

Matthay, M.A., Folkesson, H., Verkman, A.S. 1996. Salt and water transport across alveolar and distal airway epithelia in the adult lung. *Am. J. Physiol.* **270:**L487–L503

Meinild, A.K., Klaerke, D.A., Zeuthen, T. 1998. Bidirectional water fluxes and specificity for small hydrophilic molecules in aquaporins 0-5. *J. Biol. Chem.* **273:**32446–32451

Mlekoday, H.J., Moore, R., Levitt, D.G. 1983. Osmotic water permeability of the human red cells. Dependence on direction of water flow and cell volume. *J. Gen. Physiol.* **81:**213–220

Muallem, S., Zhang, R., Loessberg, P.A., Star, R.A. 1992. Simultaneous recording of cell volume changes intracellular pH or Ca^{2+} concentration in single osteosarcoma cells UMR-106-01. *J. Biol. Chem.* **267:**17658–17664

Ölveczky, B.P., Periasamy, N., Verkman, A.S. 1997. Mapping fluorophore distributions in three dimensions by quantitative multiple angle-total internal reflection fluorescence microscopy. *Biophys. J.* **73:**2836–2847

Pearce, D., Verkman, A.S. 1989. NaCl reflection coefficients in proximal tubule apical and basolateral membrane vesicles: measurement by induced osmosis and solvent drag. *Biophys. J.* **55:**1251–1259

Piston, D.W. 1999. Imaging living cells and tissues by two-photon excitation microscopy. *Trends Cell Biol.* **9:**66–69

Shi, L.B., Fushimi, K., Verkman, A.S. 1991. Solvent drag measurement of transcellular and basolateral membrane NaCl reflection coefficient in mammalian proximal tubule. *J. Gen. Physiol.* **98:**379–398

Shi, L.B., Verkman, A.S. 1989. Very high water permeability in vasopressin-dependent endocytic vesicles in toad urinary bladder. *J. Gen. Physiol.* **94:**1101–1115

Song, Y., Ma, T., Matthay, M.A., and Verkman, A.S. 2000. Role of aquaporin-4 in airspace-to-capillary water permeability in intact mouse lung measured by a novel gravimetric method. *J. Gen. Physiol.* (*in press*)

Srinivas, S.P., Bonanno, J.A. 1997. Measurement of changes in cell volume based on fluorescence quenching. *Am. J. Physiol.* **272:**C1405–C1414

Stein, W.D. 1967. The Transport of Molecules Across Cell Membranes. Academic Press, New York

Tamarappoo, B.K., Koyama, N., Gabbert, M., Verkman, A.S. 1999. High-throughput screening of combinatorial drug libraries to identify non-mercurial aquaporin inhibitors. *J. Am. Soc. Nephrol.* **10:**25*A* (*Abstr.*)

Tamarappoo, B.K., Verkman, A.S. 1998. Defective trafficking of AQP2 water channels in Nephrogenic Diabetes Insipidus and correction by chemical chaperones. *J. Clin. Invest.* **101:**2257–2267

Toriano, R., Ford, P., Rivarola, V., Tamarappoo, B.K., Verkman, A.S., Parisi, M. 1998. Reconstitution of a regulated transepithelial water pathway in cells transfected with AQP2 and an AQP1/AQP2 hybrid containing the AQP2-C terminus. *J. Membrane Biol.* **161:** 141–149

Turner, M.R., Pallone, T.L. 1997. Hydraulic and diffusional permeabilities of isolated outer medullary descending vasa recta from the rat. *Am. J. Physiol.* **272:**H392–H400

Valenti, G., Frigeri, A., Ronco, P.M., D'Ettorre, C., Svelto, M. 1996. Expression and functional analysis of water channels in stably AQP2-transfected human collecting duct cell line. *J. Biol. Chem.* **271:**24365–24370

Van Hoek, A.N., Verkman, A.S. 1992. Functional reconstitution of the isolated erythrocyte water channel CHIP28. *J. Biol. Chem.* **267:**18267–18269

Verkman, A.S. 1995. Optical methods to measure membrane transport processes. *J. Membrane Biol.* **148:**99–110

Verkman, A.S. 1998. Role of aquaporin water channels in kidney and lung. *Am. J. Med. Sci.* **316:**310–320

Verkman, A.S. 1999. Lessons on renal physiology from transgenic mice lacking aquaporin water channels. *J. Am. Soc. Nephrol.* **10:**1126–1135

Verkman, A.S., Dix, J.A., Seifter, J.L. 1985. Water and urea transport in renal microvillus membrane vesicles. *Am. J. Physiol.* **248:**F650–F655

Verkman, A.S., van Hoek, A.N., Ma, T., Frigeri, A., Skach, W.R., Mitra, A., Tamarappoo, B.K., Farinas, J. 1996. Water transport across mammalian cell membranes. *Am. J. Physiol.* **270:**C12–C30

Verkman, A.S., Wong, K. 1987. Proton NMR measurement of diffusional water permeability in suspended renal proximal tubule. *Biophys. J.* **51:**717–723

Wang, K., Ma, T., Komar, A.R., Cross, I., Frigeri, A., Verkman, A.S., Bastidas, A. 1999. Defective fluid absorption in colon of transgenic mice deficient in water channel aquaporin-4. *Gastro.* **116:***A* 944 (*Abstr.*)

Yang, B., Folkesson, H.G., Yang, J., Matthay, M.A., Ma, T., Verkman, A.S. 1999. Reduced water permeability of the peritoneal barrier in aquaporin-1 knockout mice. *Am. J. Physiol.* **276:**C76–C81

Yang, B., Verkman, A.S. 1997. Water and glycerol permeability of aquaporins 1-5 and MIP determined quantitatively by expression of epitope-tagged constructs in Xenopus oocytes. *J. Biol. Chem.* **272:**16140–16146

Yang, B., Verkman, A.S. 1998. Urea transporter UT3 functions as an efficient water channel: direct evidence for a common water/urea pathway. *J. Biol. Chem.* **273:**9369–9372

Ye, R., Verkman, A.S. 1989. Osmotic and diffusional water permeability measured simultaneously in cells and liposomes. *Biochemistry* **28:**824–829

Zhang, R., Skach, W., Hasegawa, H., van Hoek, A.N., Verkman, A.S. 1993. Cloning, functional analysis and cell localization of a kidney proximal tubule water transporter homologous to CHIP28. *J. Cell Biol.* **120:**359–369

Zhang, R., Verkman. A.S. 1991. Water and urea transport in *Xenopus* oocytes: expression of mRNA from toad urinary bladder. *Am. J. Physiol.* **260:**C26–C34